Evaluation of performance of retrofitted reinforced concrete beam column joints–a simplified model

Article *in* Asian Journal of Civil Engineering · January 2012

CITATIONS
2

READS
298

5 authors, including:

N. Lakshmanan
CSIR Structural Engineering Research Centre
195 PUBLICATIONS **1,734** CITATIONS
SEE PROFILE

Ramesh Gopal
Council of Scientific and Industrial Research (CSIR), New Delhi
29 PUBLICATIONS **88** CITATIONS
SEE PROFILE

B. H. Bharatkumar
CSIR Structural Engineering Research Centre
69 PUBLICATIONS **962** CITATIONS
SEE PROFILE

ASIAN JOURNAL OF CIVIL ENGINEERING (BUILDING AND HOUSING) VOL. 13, NO. 6 (2012)
PAGES 783-803

EVALUATION OF PERFORMANCE OF RETROFITTED REINFORCED CONCRETE BEAM COLUMN JOINTS– A SIMPLIFIED MODEL

K. Balasubramanian[a], N. Lakshmanan[b], C. Antony Jeyasehar[c],
G. Ramesh[a] and B.H. Bharatkumar[*, a]
[a]Advanced Materials Laboratory, CSIR-Structural Engineering Research Centre, Taramani, Chennai 600 113, India
[b]Wind Engineering Laboratory, CSIR-Structural Engineering Research Centre, Taramani, Chennai 600 113, India
[c]Department of Civil & Structural Engineering, Annamalai University, Annamalai Nagar- 608 002, India

Received: 10 September 2011, **Accepted**: 27 February 2012

ABSTRACT

This paper presents an experimental investigation on the behaviour of retrofitted beam-column joints subjected to cyclic loading. The beam-column joints were designed for gravity loading. The same joints were retrofitted for seismic loading with four different retrofitting strategies essentially to achieve equal strength of the segment under sagging and hogging bending moments. The results obtained from the experimental investigation gives better understanding of the strengthening and repair methodology of FRP strips, FRP sheets, MS flats and embedded additional reinforcement in RC beam–column joints under cyclic loading. A simple analytical model proposed by Ibarra et al. is shown to be an excellent tool for performance evaluation of the retrofitted beam column joints. The progressive damage in the retrofitted elements can also be well predicted.

Keywords: Cyclic; displacement; strengthening; energy dissipation; retrofitting; seismic; gravity loading

1. INTRODUCTION

Before the introduction of earthquake standards, the reinforced concrete structures were designed for gravity loading. In the earlier codes of practice, RC structures were designed to take care of vertical loads and moments, but their performance during an earthquake is doubtful. In India, most of the structures are designed for gravity loading and most of these structures are situated in seismic prone belt and hence, the existing structures need immediate

* E-mail address of the corresponding author: bharat@serc.res.in (B.H. Bharatkumar)

assessment in order to evaluate their response to earthquakes. Structures that are not designed for seismic loads require retrofit measures to avoid their collapse and huge loss of human lives. Upgradation to higher seismic zones of several cities and towns in the country has also necessitated in evolving new retrofitting strategies. In order to minimize the failure of the RC structures due to seismic event, strong column and weak beam approach has been recommended by the various codes of practice all over the world.

Beam-column joints, being the key lateral and vertical load resisting members in RC structures, are particularly vulnerable to failures in earthquakes and hence their retrofit is often the key to successful seismic retrofit strategy. In addition to horizontal excitation of the structures caused by earthquakes, vertical excitation is also produced causing additional loads on beam-column joints. It has earlier been demonstrated [1] that the degrading performance of a beam column joint can be avoided by introduction of a corner bar, where the beam reinforcement bends into the column for anchorage. The provision of a corner bar avoids the post-peak load drop due to high compressive stresses at the bend. Provision of wider column may reduce the rate of load drop in the post peak region. The repair methodologies proposed in the study include the provision of CFRP laminates and sheets. FRP is widely used in strengthening application due to its strength to weight ratio. The major benefit of FRP in strengthening application is its easy installation in any form or shape, and protection from corrosion.

Data on the performance of the retrofitted beam column joints under both compression and tension cyclic loading is very limited. This research mainly focuses on the performance of beam column joints designed for gravity loading and strengthened using four different strategies for seismic loading. The gravity loaded beam column joints were retrofitted with various retrofitting strategies and the behaviour of strengthened joints under compression and tension cyclic loading was studied. The experimental investigation on the performance of the four retrofit methodologies adopted to strengthen the beam column joints is critically compared using an analytical model developed by Ibarra et al. [19]. This paper presents the experimental investigation carried out to study the behaviour of seismic retrofitted beam column joints under cyclic loading and the analytical model to predict the number of cycles to failure. Based on the model one can evaluate the efficiency of retrofitting technique.

In order to predict the number of cycles to failure and total energy absorption capacity, a hysteretic model that includes strength and stiffness deterioration properties has been used in the present study. The model incorporates an energy based deterioration parameter that controls the cyclic deterioration modes: basic strength and post capping strength deterioration. The last hysteresis curve is assumed as the failure cycle, from which the failure deflection is evaluated. The cyclic deterioration parameters have been predicted based on the hysteretic model. The predicted cyclic deterioration parameters have been verified with the experimental results.

2. LITERATURE SURVEY

In order to retrofit/strengthen existing structural elements, section enlargement by concrete jacketing and steel plate bonding are used to achieve the required performance [2-4]. The above mentioned technique is a passive confinement type. In this method, concrete starts to dilate first and expands laterally due to which the concrete/steel jacketing restrains the dilation as a result of high compressive strain that is induced [5].

Comprehensive literature survey has been carried out by Murat [6] pertaining to the performance of various repair and strengthening techniques, such as, epoxy repair, concrete jacketing, steel jacketing, and FRP jacketing to improve the seismic performance of non seismically designed RC beam column joints. They concluded that(i) model testing carried out on 1/3 to $1/8^{th}$ scale models may not simulate the actual behaviour (ii) epoxy repair techniques have limitations, (iii) concrete and steel jacketing though effective, are labour intensive and require engineering expertise, and (iv) among all the repair techniques, externally bonded FRP composites appear to be the best option. Finally they opined that the present state of knowledge is inadequate on repair techniques and their design.

Guimaraes et al. [7] concluded that in high strength concrete for 4% drift level, the ratio of measured to calculated joint shear strength vary between 1.21 to 1.69. The failure of beam column joint took place after the 4% drift level and formation of plastic hinge in the beam. Li et al. [8] observed the behaviour of RC beam column joints strengthened by hybrid FRP under monotonic loading. It is well known that considerable increase in stiffness and load carrying capacity can be achieved by repair measures. The gravity load design and seismic design without ductile detailing possess low energy dissipation capacity (Sasmal et al.) [9,10 &11]. In beam column joint, the failure occurred in the joint region and joint shear stress was more predominant in the joint.

Behaviour of FRP composites confined concrete members subjected to cyclic flexure with and without axial compression was presented by Nanni and Norris [12]. In the study, two types of FRP viz., braided aramid and pre-formed glass-aramid were used. It was reported that flexural strength and ductility were enhanced by the use of FRP confinement. Moderately damaged beam column joint strengthened with FRP strips under shear showed moderate success and the same joint injected using epoxy improved the effectiveness of repair scheme (Shrestha, et al.) [13]. Tsonos [14] conducted a series of tests to determine the effectiveness of the manual guidelines of the United Nations Industrial Development Organization (UNIDO) for the repair and strengthening of beam-column joints damaged by severe earthquakes. Their study concluded that addition of externally bonded FRP composites can enhance not just the shear capacity but the deformation and energy absorption capacity of the connection. Simulated seismic load tests were performed on exterior joint model strengthened with FRP. There is a significant increase in strength, energy dissipation and stiffness characteristics compared to the unstrengthened beam (Tsonos et al.) [15].

Interior beam-column joints representing pre-seismic code design were taken by Salloum et al. [16]. The four joints were cast with no transverse reinforcement in the joint shear portion. Two beam-column joints were strengthened with CFRP sheets in the shear zone and they were effectively prevented against debonding through mechanical anchorages. All the beam-column joints were subjected to cyclic lateral loading similar to earthquake loading. The

strengthened joints exhibited good improvement in joint shear and increase in ductility.

Cyclic tests were carried out on cruciform beam-column joint specimens, with two different configurations of geometry and various configuration of strengthening by externally bonded FRP fabric by Ayala et al. [17]. The specimens were designed for gravity loading, but no seismic design was considered. They mainly focused on a possible worst case scenario for pre-seismic design deficiencies such as plain round bar, mild steel reinforcement, inadequate transverse links in the joint core, weak concrete and strong beam/ weak column. The deficient joints were strengthened with CFRP sheets and strips. They concluded that the CFRP wrapping was more suitable for diagonal wrapping and enhances the confining action of the concrete at the joint corners. The addition of vertical CFRP strips in the joint region increases the shear capacity.

The earlier investigations have claimed the effectiveness of using FRP sheets for the retrofit of RC structures which have non seismic detailing. However, since the seismic forces involve reversal of loading, the present study aims at studying the performance of retrofitted beam column joints under reversed cyclic loading.

3. EXPERIMENTAL INVESTIGATION

Considering the various repair techniques, it becomes necessary to have a comparative evaluation of the repair strategies. Performance parameters have been suggested by Lakshmanan [21-22] based on equivalence of deformation, equivalence of energy and damping factor based on energy absorption under monotonic loading. Similar performance parameter is needed to evaluate the various repair strategies under reversed cyclic loading. This paper suggests one methodology which is simple and easy to handle for such performance evaluation. The present study envisages the development of different types of retrofitting methodology for non-seismically designed beam-column joints. The evaluation of performance of retrofitted beam column joints under cyclic loading and its validation with analytical model is presented.

The experimental program consisted of testing four RC beam-column joint specimens. The columns had a cross section of 200 mm x 200 mm with an overall length of 2100 mm and the beams had a cross section of 200 mm x 200 mm with a length of 750 mm. The concrete mix was designed for a target strength of 40 MPa at the age of 28 days. The longitudinal reinforcement of the square columns was kept constant for all the RC beam-column joint specimens and consisted of 4 numbers of 12mm diameter (HYSD) bars having an yield strength of 500 MPa. The spacing of 6mm dia mild steel stirrups in columns was 200 mm c/c as per IS 456:2000 [18] as required by the gravity design (Figure 1). In the beam portion, main reinforcement consisted of two numbers of 16mm HSD bars. Two numbers of 10mm dia HSD bars provided as stirrup hangers also perform as compression reinforcement. The stirrup spacing in the beams was 150mm c/c. In addition to the above, a corner bar of 16mm dia was provided in the column portion as shown in Figure 2.

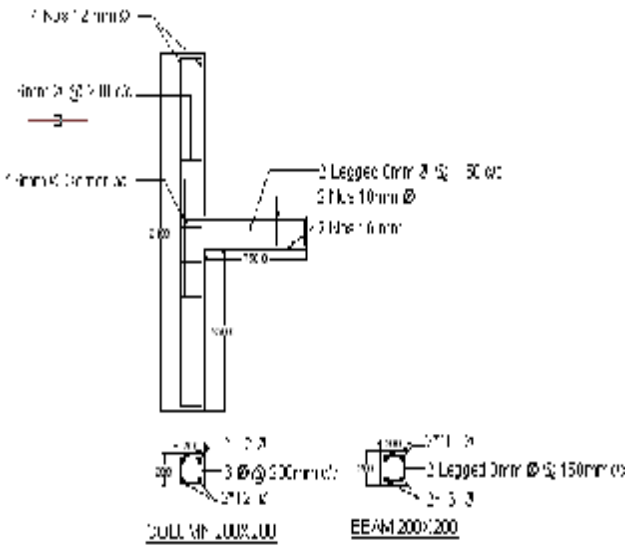

Figure 1. Reinforcement details of beam-column joint

Figure 2. View of reinforcement grills with corner bars

3.1 Strengthening of RC beam-column joint specimens

The aim of the repair methodology was to provide equal flexural strength in beam for both downward and upward loading (Figure 1). Additional reinforcements using CFRP laminates/ sheets, reinforcing bars and steel plates were added using different techniques to achieve this objective. The beam column joints cast were retrofitted with four different methodologies as detailed below.

1. Providing CFRP laminates in the top face of the beam (Method 1)
2. Providing CFRP laminates in the top face of the beam and confining the junction with CFRP sheets (Method 2)
3. Providing MS flat section in the top face of the beam, anchored with MS bolts on both faces (Method 3)
4. Providing additional reinforcement in the top face by cutting a groove and filling the groove with non-shrink cementitious material and confining the joint with CFRP sheets (Method 4)

3.2 Properties of CFRP sheets and laminates

CFRP fabric: is a unidirectional, stitched, carbon fiber fabric to be used with impregnated resin. Tensile strength, elastic modulus and elongation at breakage of the dry fiber are 4200 MPa, 242,000 MPa and 1.55%, respectively. Fiber density is 230 GSM. Impregnated fibers are assumed to have a thickness of 1 mm per layer with elastic modulus of 40,000 MPa.

CFRP laminate: Carbon fiber laminates are produced by pultrusion process. The width and thickness are 50 mm with 1.4 mm. Elastic modulus, tensile strength and elongation at break of the laminate are 165,000 MPa, 2800 MPa and 1%, respectively.

Method 1

In method –1, the beam-column specimen is strengthened with CFRP laminates on the top face of the beam as shown in Figure 3. The sides of the beam at top were ground to a width of 50mm and to a depth of 3mm using a grinding machine. The grounded surface was thoroughly cleaned to be free from dirt, oil and grease. One coat of primer was applied on the ground surface for effective bond between laminate and concrete. The 50 mm wide CFRP laminate was cleaned with acetone and three holes of 12 mm diameter was drilled for fixing the laminate into the concrete surface. The saturant was then applied over the surface of the beam and laminate face. The CFRP laminates was bonded on the beam surface and allowed to cure for seven days. Three 12mm dia bolts were also fixed using epoxy to increase mechanical anchorage of CFRP laminate.

Method 2

In this retrofit methodology, in addition to the provision of the CFRP laminate as described in Method 1, the joint region was confined with CFRP sheets in the joint area as shown in Figure 4. Before bonding the FRP sheets, the specimen was cleaned to remove the surface laitance. One coat of primer was applied on the cleaned surface. CFRP sheets were saturated with two component saturant fully before applying it to the surface. Finally the saturated CFRP sheets were bonded in the surface and rolled with roller to remove any air voids and allowed to cure for seven days.

Method 3

The CFRP laminate in the method 1 was replaced with a steel flat of 40mm width and 4mm thickness in this retrofit methodology. The details of the strengthened beam-column joint is shown in Figure 5.

Method 4

In this method, additional reinforcement of 12mm dia bar was inserted in the top face of the beam. In order to insert the 12mm bar, a groove of 25mm depth upto the level of existing reinforcement was cut. The groove was continuous from the front face of the beam, the exterior side of the column and the rear face of the beam (Figure 6). The additional reinforcing bar was also continuous in the form of ‘U’- shape and went around the column reinforcement. The additional reinforcement bar was tack welded to the existing reinforcements. Then the groove was covered with a non-shrink micro concrete. After the provision of the additional compression reinforcement, the beam-column joint was confined by CFRP sheets in the beam column joint location as explained in Method 2. The schematic representation of Method 4 is shown in Figure 6.

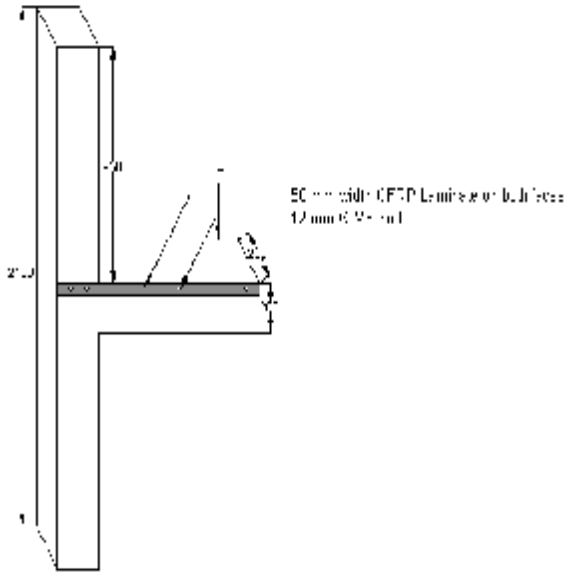

Figure 3. CFRP laminates in the top face of the beam

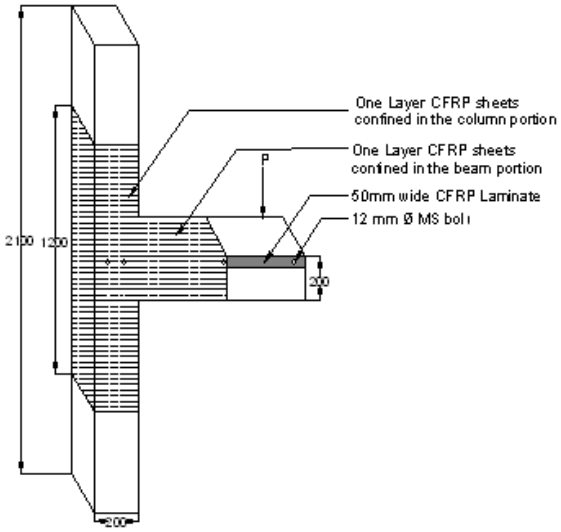

Figure 4. CFRP laminates in the top face of the beam and confined in junction with CFRP sheets

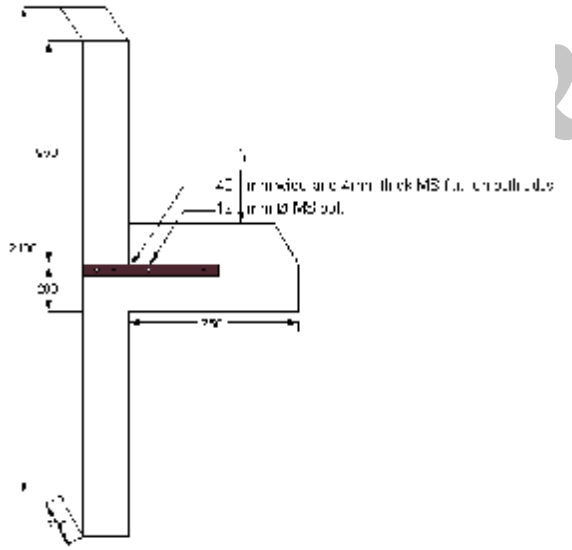

Figure 5. MS flat section in the top face of the beam

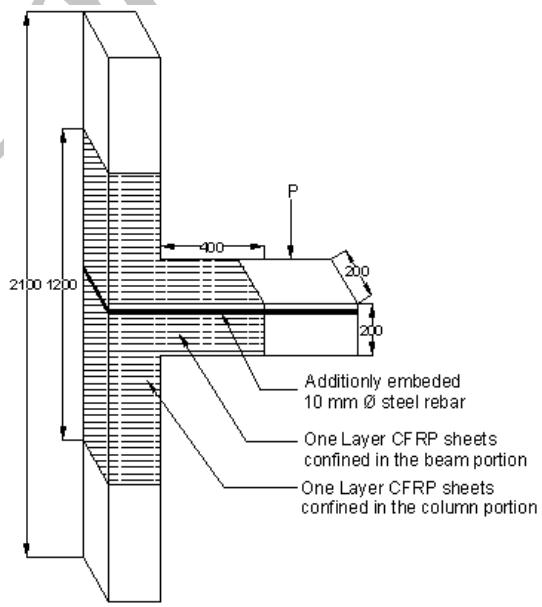

Figure 6. Additional reinforcement in the top region of the beam and confined in junction with CFRP sheets

3.3 Experimental test setup and loading arrangement

The test set up was arranged on a heavy duty test floor so that the beam-column joint rested on the floor and the cyclic load was applied in the plane of the test floor. The column ends were loaded to a predefined axial load through a hydraulic jack resting on test floor. A 500 kN load

cell was mounted at one end of the column to measure the axial load response from the column. A permanent axial load of 300 kN was applied to the column through the jack positioned between the column and one of the reaction bulk heads at the start of the test. The schematic diagram of the test set up is shown in Figure 7.

The beam was loaded using a 250 kN servo-hydraulic actuator under displacement control in both compression and tension modes. The displacement at yield of the main reinforcement for downward loading as obtained on companion specimens without repair was 5 to 6mm. Hence a displacement increment of 5mm in both sagging and hogging flexural load cycles was maintained till failure. In each load cycle, three cycles were repeated. Since the testing was carried out using a servo controlled actuator, the rate of loading was fixed at 2 mm per minute for the first cycle and for the subsequent cycles, it was increased to reduce the total duration of testing. The first cycle of loading introduced tensile strain at the bottom face of the beam. Displacement was measured at free end of the beam using an LVDT. The output from the actuator and displacement from the LVDT was acquired in a data logger at a frequency of 1Hz. The same was stored in a dedicated computer system for further analysis.

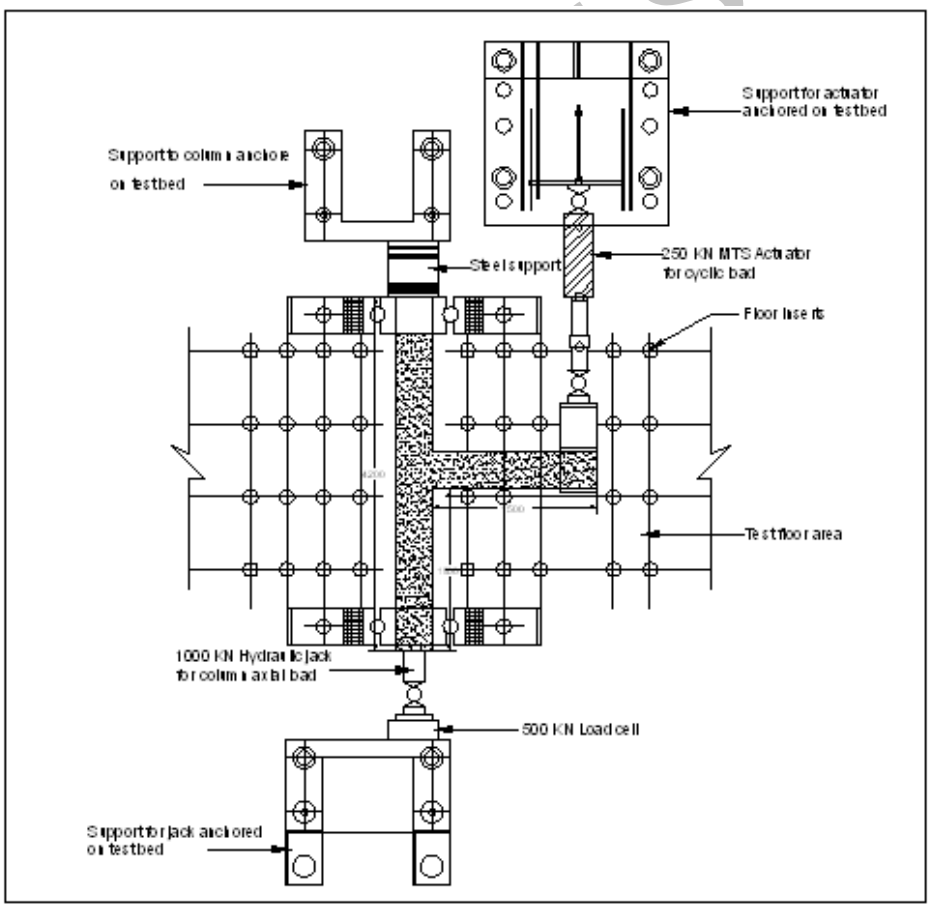

Figure 7. Typical test setup

4. EXPERIMENTAL RESULTS

Details of the typical Time vs Displacement plot for different strengthening schemes are given in Figure 8. The load deflection plots for the retrofitted beam column joints using the various methodologies are given in Figure 9.

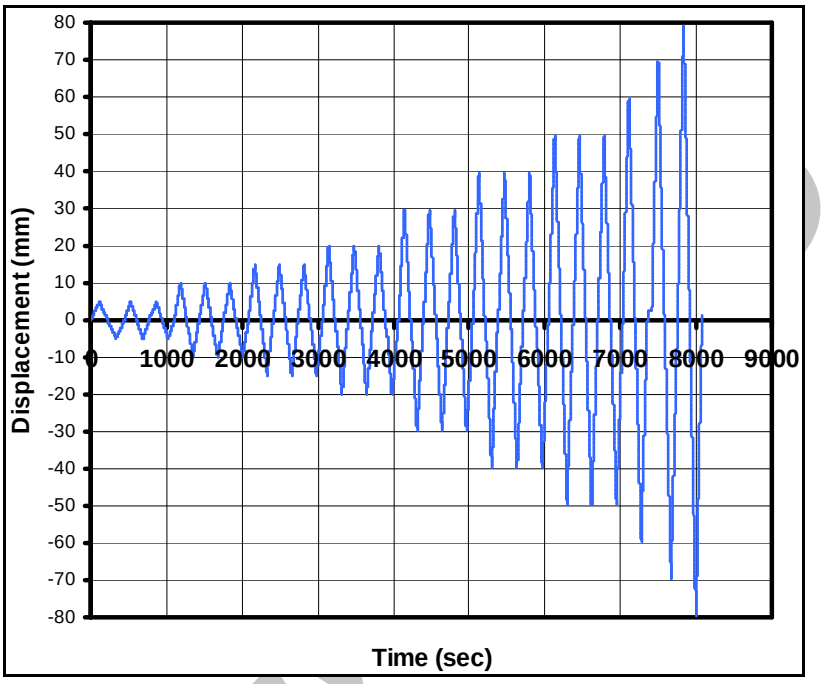

Figure 8. Typical time vs displacement plot for different strengthening schemes

In the case of the repair Method 1, the strengthening was carried out in the top face of the beam using CFRP laminate. During the test, the cyclic response in the tension and compression faces showed significant improvement upto a displacement of 20 mm. Beyond 20 mm, the repaired face showed extensive cracking in the laminate portion and further enhancement of the load was not achieved. After this stage, the joint was loaded only on the bottom face till failure. The primary mode of failure was debonding of the FRP strips in the joint region as shown in Figure 10a. The 12mm bolt meant for anchoring also pulled out near the inner edge of the column due to crushing of concrete in that region. Beyond this stage, the joint was loaded only from bottom till failure as shown in Figure 10(a). The beam failed around 60mm upward displacement.

In the case of the repair Method 2, the strengthening has been carried out using CFRP laminate in the top face of the beam and further confining the junction with CFRP sheets. During the reversed cyclic loading, it was observed that confining the joint with CFRP did not result in significant improvement in the load carrying capacity of the joint. Beyond 30 mm, the top face showed extensive spalling of concrete in the laminate portion and further enhancement of the load was not achieved. Concrete spalling was also observed at the beam–column joint on the face of the column as well. The column wrap which secured the ends of

the FRP strip prevented the strip from completely debonding; however, the column wrap was not effective in preventing localised debonding in the joint region. The final crack pattern in the joint region is shown in Figure 10b.

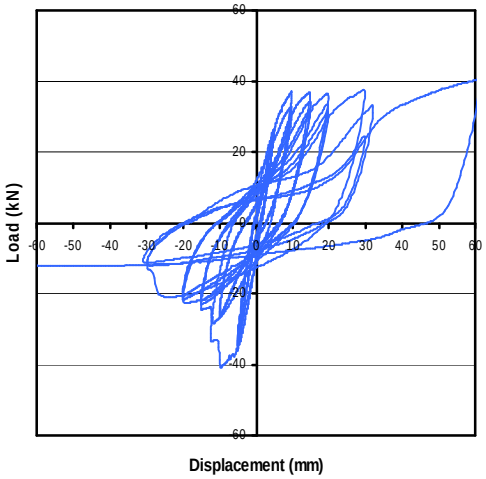

(a) CFRP laminate

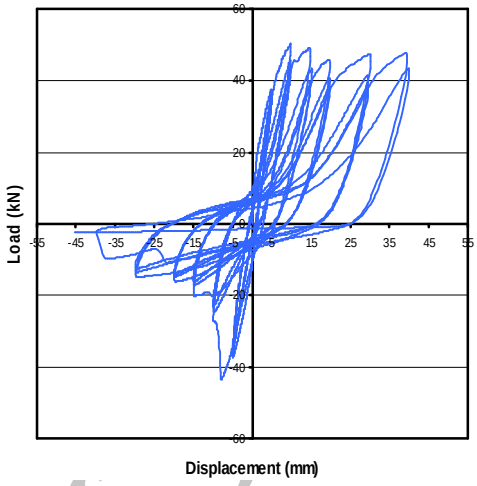

(b) CFRP laminate and confined with CFRP sheet

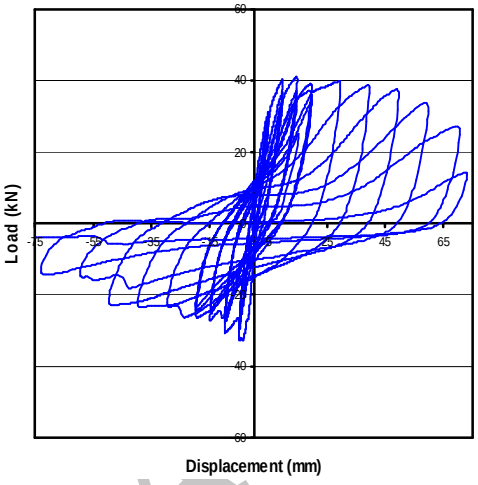

(c) 50mm wide MS flat

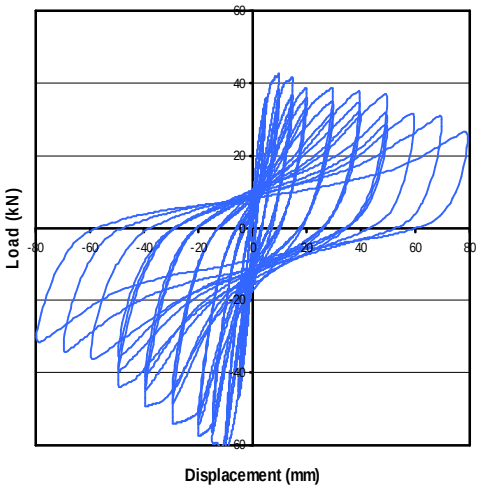

(d) Embedded additional reinforcement and confined with CFRP sheets

Figure 9. Cyclic behaviour of beam-column joints

In the case of the repair Method 3, the strengthening has been carried out using MS flat section in the top face of the beam. Even though the load carrying capacity of the joint was marginally lower compared to methods 1 and 2, the ductility of the joint was improved as seen from Figure 9c. After reaching 50mm displacement, only one load cycle was carried out with incremental amplitude being 10mm. Beyond 70 mm displacement cycle, the plate reinforcement in the joint could not sustain the loading as the concrete has completely spalled leading to loosening of the anchor bolts. The ductility

of the joint was significantly improved with the provision of the MS flat compared to the earlier two methods and the retrofit methodology adopted was better. The failure pattern of beam column joint is shown in Figure 10c**.**

(a) CFRP laminate

(b) CFRP laminate and confined with CFRP sheet

(c) 50mm wide MS flat

(d) Embedded additional reinforcement and confined with CFRP sheets

Figure 10. Failure pattern of various strengthened beam column joints

The strengthening has been carried out using additional reinforcement in the top region of the beam in Method 4. In addition to the additional reinforcement, CFRP sheets were wrapped in the joint region for further confinement. There was a sharp increase in the load carrying capacity, ductility and energy absorption capacity of the joint compared to other three methodologies adopted. Concrete crushing was also observed at the beam–column joint on the

compression face of the column. The column FRP wraps secured the additional reinforcement completely in position even after the failure of joint/non shrink grout. The column wraps were effective in confinement of the joint region. The final failure pattern in the joint region is shown in Figure 10d. After reaching 50mm displacement, only one load cycle was carried out with incremental amplitude of 10mm.The joint did not fail even after achieving a displacement level of 80 mm and continued to carry 40% of the peak load. This retrofitting methodology shows significant improvement in the load carrying capacity and overall performance.

5. ANALYTICAL PREDICTION

In the present investigation, performance of the retrofitted beam-column joints using the four retrofit methodologies have been evaluated under cyclic loading. In order to predict the failure deformation and the total cumulative energy dissipation capacity of the specimens, hysteretic model proposed by Ibarra et al. [19] has been used. This model is relatively a simple hysteretic model that includes strength and stiffness deterioration properties, features that are critical for demand predictions as the structural systems approach collapse. This model incorporates an energy based deterioration parameter that controls the cyclic deterioration modes: basic strength, post - capping strength deterioration.

5.1 Back bone curve

The backbone curve defines the monotonically increasing deformation response for all the hysteretic models considered in this study (Figure 11). If no deterioration exists, the backbone curve is defined by three parameters: the elastic (initial) stiffness K_e, the yield strength Fy, and the strain-hardening stiffness $K_s = \alpha_s K_e$. If deterioration of the backbone curve is included, a softening branch begins at the cap deformation (δ_c), which corresponds to the peak strength (F_c) of the load- deformation curve. If δ_c is normalized by the yield deformation, the resulting ratio may be denoted as ductility capacity (δ_c/δ_y). The softening branch is defined by the post-capping stiffness, $K_c = \alpha_c K_e$, which usually has a negative value. In addition, a residual strength can be assigned to the model, $F_r = \lambda F_y$, which represents the fraction of the yield strength of the component that is preserved once a given deterioration threshold is achieved. When such a residual strength is specified, the backbone curve is supplemented with a horizontal line of ordinate F_r, and the strength will not drop below this value, i.e. the residual strength is not modified when cyclic deterioration shrinks the backbone curve.

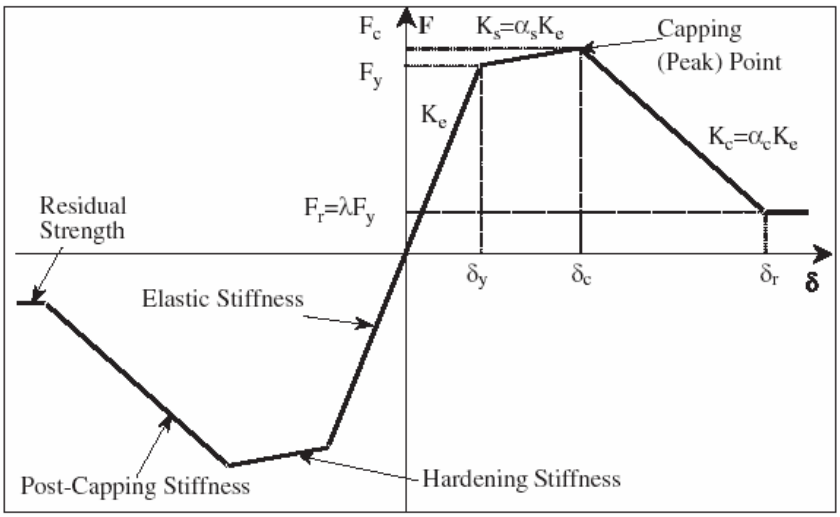

Figure 11. Back bone curve for hysteretic models

The parameters α_s, δ_c/δ_y, α_c, and λ are obtained either from analytical predictions or from calibration of the hysteretic models with load–deformation data obtained from experiments. The hysteretic models allow these parameters to have different values in the positive and negative directions.

5.2 Cyclic strength and stiffness deterioration based on hysteretic energy dissipation

Four cyclic deterioration modes may be activated once the yield point is surpassed in at least one direction: basic strength, post-capping strength, unloading stiffness, and reloading stiffness deterioration. The cyclic deterioration rules are the same for all the hysteretic models with the exception of the accelerated stiffness deterioration, which does not exist in the bilinear model. It is hypothesized that all the repaired beam elements basically have similar hysteretic behaviour appears logical to predict the hysteretic behaviour, and hence is chosen for further analysis. Second and third cycles only showed very marginal decrease in strength, and no reduction in stiffness. Hence only primary cycles are considered for analysis. The peak-oriented model will be used to illustrate the effect of cyclic deterioration.

The cyclic deterioration rates are controlled by the rule developed by Rahnama and Krawinkler [20], which is based on the hysteretic energy dissipated when the component is subjected to cyclic loading. It is assumed that every component possesses a reference inherent hysteretic energy dissipation capacity, regardless of the loading history applied to the component.

The cyclic deterioration in cycle 'i' is defined by the parameter β_i, which is given by the following expression:

$$b_i = \left(\frac{E_i}{E_t - \sum_j^i E_j} \right) \tag{1}$$

Where, E_i is the hysteretic energy dissipated in cycle i, ΣE_j is the hysteretic energy dissipated in all previous cycles through loading in both positive and negative directions, E_t is the reference hysteretic energy dissipation capacity ($E_t = \gamma F_y \delta_y$). The parameter γ expresses the hysteretic energy dissipation capacity as a function of twice the elastic strain energy at yielding ($F_y\delta_y$) and it is calibrated from experimental results and can be different for each deterioration mode. Finally, c is the exponent defining the rate of deterioration. Rahnama and Krawinkler suggest that a reasonable range for c is between 1.0 and 2.0. If the displacement history consists of constant amplitude cycles, a unit value for c implies an almost constant rate of deterioration. For the same displacement history, a value c = 2 slows down the rate of deterioration in early cycles and accelerates the rate of deterioration in later cycles.

Throughout the loading history, βi must be within the limits $0< \beta_i \leq 1$. If β_i is outside these limits ($\beta_i \leq 0$ or $\beta_i > 1$), the hysteretic energy capacity is exhausted and collapse is assumed to take place. Mathematically,

$$\gamma F_y \delta_y - \sum_{j=1}^{i} E_j < E_i$$

The individual modes of deterioration are described below.

The reduced strength and stiffness in successive load cycles is taken as and a typical strength deterioration model is shown in Figure 12.

$$F_i = F_{i-1}\,(1-\beta_i) \tag{2}$$

$$K_i = K_{i-1}\,(1-\beta_i) \tag{3}$$

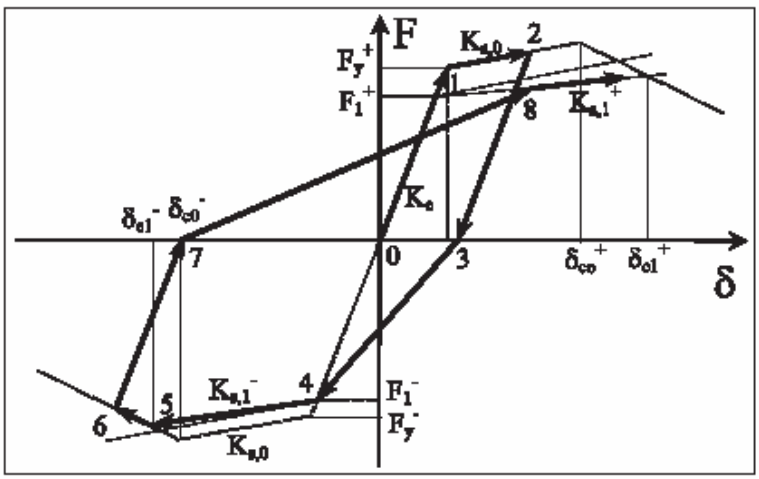

Figure 12. Typical basic strength deterioration

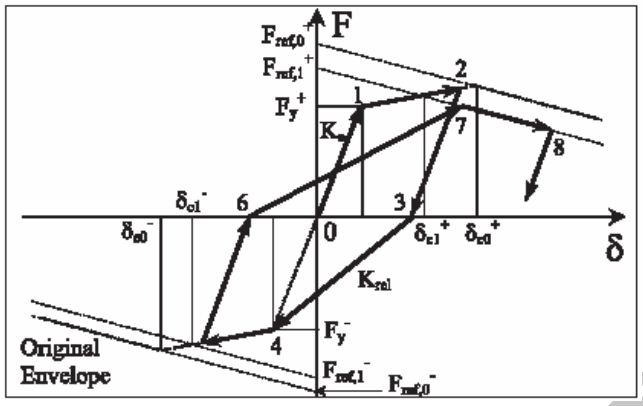

Figure 13. Typical post-capping strength deterioration

A typical post capping strength deterioration model is shown in Figure 13. Since the specimen had equal strength in a marginal modification was made to the model as given below. The total energy absorption is taken as

$$\gamma_t = (\gamma/2 + f\,\gamma/2)\,\delta_y\,F_y \qquad (4)$$

Where f = a factor

= (Peak load for –ve direction/Peak load for +ve direction)

Thus $F_i = F_{i-1}\,(1-\beta_i)$ in the stronger direction, and

$F_i = f\,F_{i-1}\,(1-\beta_i)$ in the weaker direction.

The displacement are $\pm\, n\,\delta_y$ at any given load cycle, where n is an integer. The value of γ is chosen by trial and error to obtain a best fit.

6. COMPARISION OF ANALYTICAL PREDICTION WITH EXPERIMENTAL RESULTS

While the initial stiffness in all the models were more or less constant, the values of α_s and α_c have been chosen as given in Table 1. The yield load taken as corresponding to a deflection of 5mm varied in the range of 38 to 39 kN for specimens 2, 3 and 4, and was only 32kN for specimen-1. The cyclic deterioration factor c is assumed as 1.3. The analytical prediction of the hysterisis loop was obtained by trial and error method by varying the γ, which is used in the calculation of E_t, the reference hysteretic energy dissipation capacity ($E_t = \gamma F_y \delta_y$). The hysteretic energy capacity is exhausted and collapse is assumed to take place when, β_i is outside limits ($\beta_i \leq 0$ or $\beta_i > 1$). The last hysteresis curve is the failure cycle, from which the failure deflection can be evaluated. Typical experimental and predicted load deflection plots are given in Figures 14.

Table 1: Basic parameters used for cyclic deterioration model

ID	Yield load, kN	Peak load, kN	α_s	α_c	γ
Control	30.0	35.1	0.319	-0.490	15
Method 1	30.9	36.3	0.327	-0.044	26
Method 2	38.8	50.0	0.375	-0.033	28
Method 3	37.1	39.4	0.083	-0.001	90
Method 4	37.1	42.3	0.401	-0.016	48

The Process of analysis clearly reveals that the post peak load drop leading to negative stiffness indicated by the value of α_c and the value of γ the energy absorption capacity are the most significant parameters that affect the hysteretic behaviour. The post yield- pre peak stiffness α_s would be an important only if considerable displacement takes place in this region. As it is, the peak occurred at twice the value of the yield displacement, and hence α_s has limited role in predicting hysteretic behaviour. A lower magnitude of α_c indicates slower rate of strength degradation under monotonic loading. Lower rate of load drop is definitely advantageous. Based on the analysis of test data, repair methodology-1 is least effective and methodology-3 is most effective. It is interesting to note that the methodology-1 uses CFRP laminate and methodology-3 uses steel plate, both anchored using bolts. The location of the bolt was close to the beam-column face which got crushed making the bolt ineffective to anchor CFRP laminate in methodology-1. In the methodology -3, all the anchor bolts were beyond the potential damage region as can be seen from Figure 10.

The bolts are to be positioned in the column between the outer face and 0.5 times the width of the column. Stress concentration in re-entrant corners at the beam-column interface is more susceptible to crushing of concrete under cyclic loading. The method 4 which suggests embedded additional steel reinforcement confined with CFRP sheets gives good performance and can be carried out effectively in the field without too much dependence on expertise and detailing. The variation of β with deflection indicates the build-up of damage. The build-up of damage is non-linear and once the value exceeds 0.5 it quickly builds up leading to failure as can be seen from Figure 15. The control specimen cyclic behaviour has been evaluated based on monotonic test conducted and reported elsewhere [1] using α_c as -0.490 and γ as 15. Two performance parameters are suggested.

$$Cp_1 = \frac{\text{Deformation at 25\% (or) 50\% Beta value of repaired specimen}}{\text{Deformation at 25\% (or) 50\% Beta value of control specimen}}$$

$$Cp_2 = \frac{\text{Energy absorbed at failure of repaired specimen}}{\text{Energy absorbed at failure of control specimen}}$$

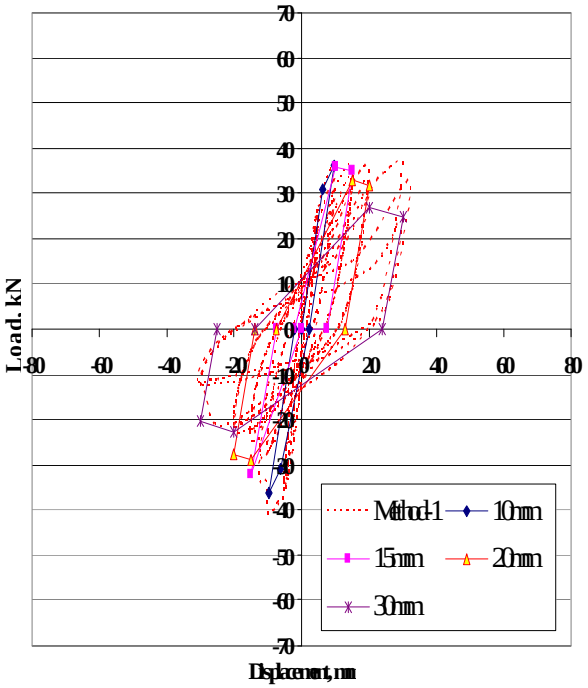

(a) CFRP laminate

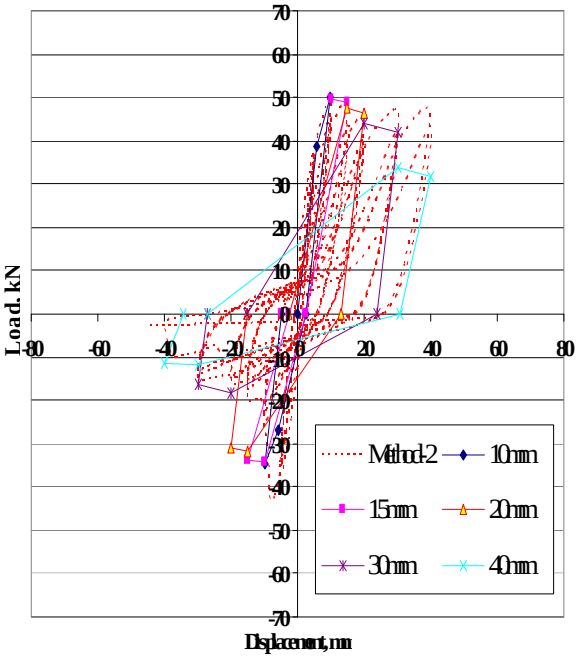

(b) CFRP laminate and confined with CFRP sheet

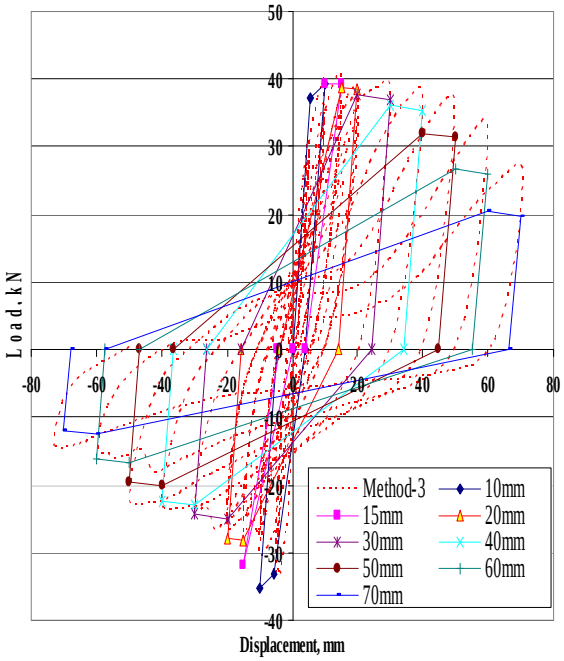

(c) 50mm wide MS flat

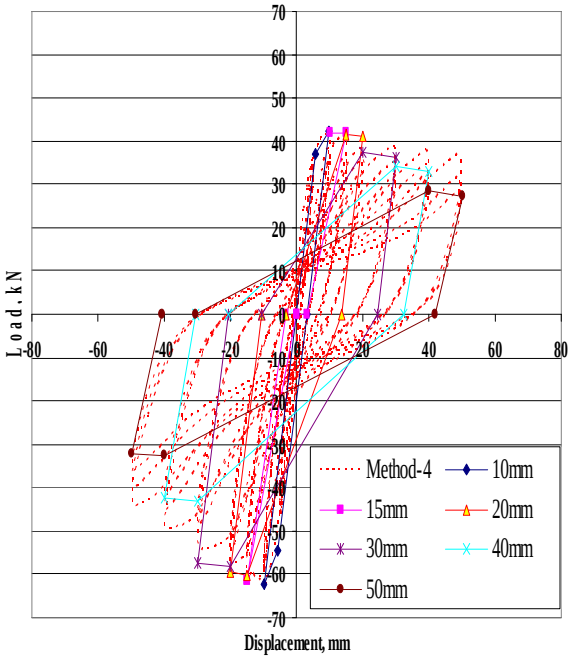

(d) Embedded additional reinforcement and confined with CFRP sheets

Figure 14. Load-deflection response for cyclically loaded various strengthening schemes

The performance parameters are given in Table 2. The values of Cp_1 and Cp_2 are very close in all the cases indicating that the normalized profile of β variation with (δ/δ_f) may be a constant. Figure 15 shows the non-dimensional plot of β vs (δ/δ_f) for all specimens, and they are very similar. Expressing $\beta = (\delta/\delta_f)^n$ the value of n is obtained as 2.5 as shown in Figure16. Thus the ratio of failure deformation between the retrofitted specimen and the control specimen for cyclic loading defines a unique performance parameter. This is exactly similar to the concept of ductility enhancement under monotonic loading, which can be used as performance parameter.

Table. 2 Performance parameters

ID	Cp_1 (25%)	Cp_1 (50%)	Cp_2	$Cp=(\delta/\delta_f)$
Control	1.00	1.00	1.00	1.00
Method 1	1.18	1.18	1.74	1.18
Method 2	1.52	1.50	1.79	1.50
Method 3	2.98	3.00	6.20	3.00
Method 4	1.83	1.87	4.45	1.90

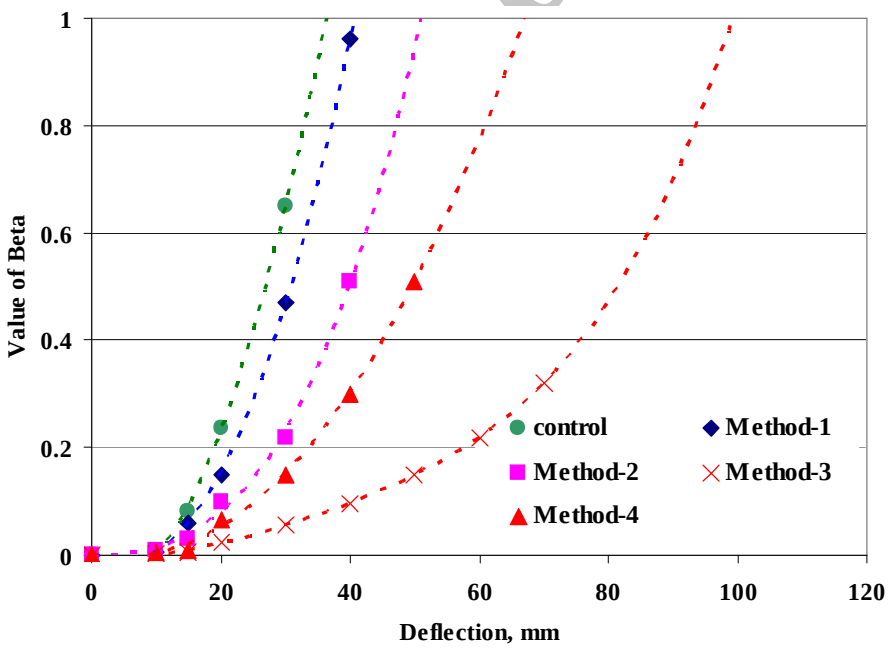

Figure 15. Variation of beta values with respect to deflections

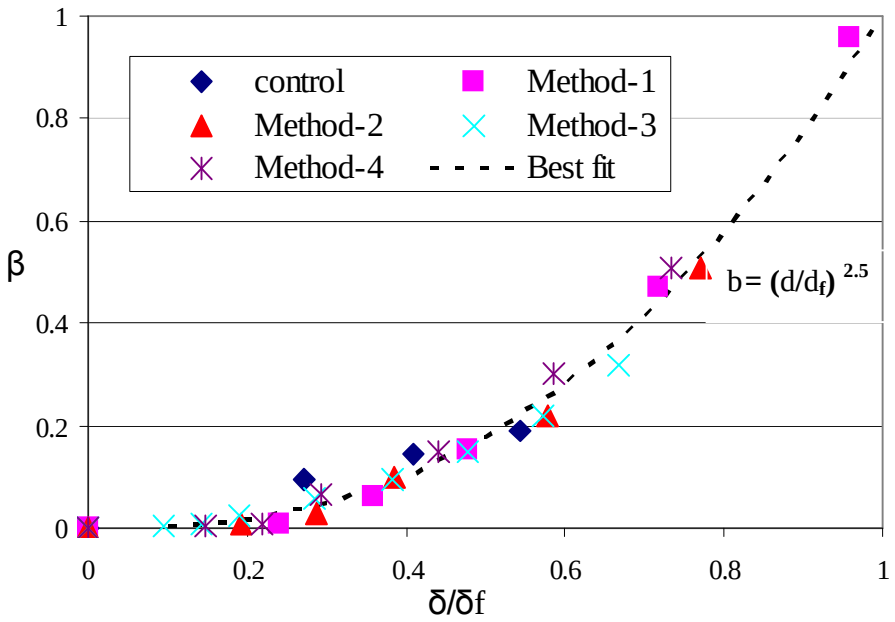

Figure 16. Variation of beta values with (δ/δ_f)

7. CONCLUSIONS

Four repair strategies have been formulated for enhancing the seismic performance. Cyclic load testing under reversed cyclic loading is a good candidate for performance evaluation of various repair strategies. A simple methodology is required to quantitatively estimate the improvement provided by various strategies. The cyclic deformation behaviour predicted from the simple model using hysteretic energy and incremental damage compares well with experimental results. Two performance parameters have been suggested for evaluation of repair methodologies. The location of anchor bolts plays a significant role in improving the efficiency of the repair methodology. The damage parameter β varies uniquely with non-dimensionalised parameters (δ/δ_f) for all the repaired specimens. Repair strategies (3) and (4) tested have shown superior performance.

Acknowledgement: This paper is being published with the kind permission of the Director, CSIR-SERC The authors sincerely thank the staff of Advanced Materials laboratory and Structural Testing Laboratory, CSIR-SERC, Chennai for their help during testing of specimens and encouragement during all the phase of this work.

REFERENCES

1. Balasubramanian K, Lakshmanan N, Antony Jeyasehar C, Krishnamoorthy TS, Bharatkumar BH. Behaviour of reinforced concrete beam column joint retrofitted with carbon fibre reinforced polymer warp, Journal of 3R's (Repair Restoration and Renewal

of Built Environment), No. 4, **1**(2010) 170-8.
2. Priestley MJN, Seible F, Xiao Y, Verma R. Steel jacket retrofitting of reinforced concrete bridge columns for enhanced shear strength–Part 1: Theoretical considerations and test design, *ACI Structural Journal,* No. 4, **91**(1994) 394–405.
3. Priestley MJN, Seible F, Xiao Y, Verma, R. Steel jacket retrofitting of reinforced concrete bridge columns for enhanced shear strength–Part 2: Test results and comparison with theory, *ACI Structural Journal,* No. 5, **91**(1994) 537–51.
4. Priestley, MJN, Seible F. Design of seismic retrofit measures for concrete and masonry structures, *Construction Building Materials,* No. 6, **9**(1995) 365–77.
5. Said A, Nehdi M. Rehabilitation of RC frame joints using local steel bracing, *Structural Infrastructure Engineering: Maintenance Manage Life-cycle Des Perform,* No. 6, **4**(2008) 431–47.
6. Murat E, Kahn LF, Zureick AH. Repair and Strengthening of Reinforced Concrete Beam-Column joints: State of the Art, *ACI Structural Journal,* No. 2, **102**(2005) 1-14.
7. Guimaraes GN, Kreger ME, Jirsa, J.O. Evaluation of Joint Shear Provisions for Interior Beam-Column-Slab connections using high-strength materials, *ACI Structural Journal,* (1992) 89-98.
8. Li J, Samali B, Ye L, Bakoss S. Behaviour of concrete beam–column connections reinforced with hybrid FRP sheet, *Composites Structures,* Nos. 1-4, **57**(2002) 357–65.
9. Sasmal S, Lakshmanan, N, Ramanjaneyulu K, Nagesh R. Iyer, Balthasar Novák, Srinivas V, Saravana Kumar K, Constanze Roehm. Development of upgradation schemes for Gravity Load Designed Beam Column sub-assemblages under Cyclic Loading, *Construction and Building Materials,* **25**(2011) 3625-38.
10. Sasmal S, Balthasar Novák, Ramanjaneyulu K, Constanze Roehm, Srinivas V, Lakshmanan, N, Nagesh R. Iyer. Üpgradation Gravity Load sub-assemblages subjected to Seismic Type of Loading, *Composite Structures,* **93**(2011) 1561-73.
11. Sasmal S, Ramanjanayulu K, Balthasar Novák, Srinivas V, Saravana Kumar K, Christian Korkowski, Constanze Roehm, Lakshmanan, N, Nagesh R. Iyer. Seismic Retrofitting of Non ductile Beam Column sub Assemblages using FRP wrapping and Steel plate Jacketing, *Construction and Building Materials,* **25**(2011) 175-82.
12. Nanni A, Norris MS. FRP jacketed concrete under flexure and combined flexure compression, *Construction and Building Materials,* No. 5, **9**(1995) 273-81.
13. Shrestha R, Smith ST, Samali B. The Effectiveness of FRP strips in repairing moderately and severely damaged R.C beam column connections, *Magazine of Concrete Research,* No. 9, **63**(2011) 629-44.
14. Tsonos AG. Lateral load response of strengthened reinforced concrete beam-column Joints, *ACI Structural Journal,* No. 1, **96**(1999) 46-56.
15. Tsonos AG, Stylianidis KA. Pre-seismic and post-seismic strengthening of reinforced concrete structural sub-assemblages using composite materials (FRP), *Proceedings of 13th Hellenic Concrete Conference,* Rethymno, Greece, vol. 1, 1999, pp. 455-466 [in Greek].
16. Yousef A, Al-Salloum Tarek H, Almusallam. Seismic response of interior RC beam-column joints upgraded with FRP sheets. I: Experimental study, *Journal of Composites for Construction, ASCE,* No. 6, **11**(2007) 575–89.

17. D'Ayala D, Penford A, Valentini S. Use of FRP fabric for strengthening of Reinforced concrete beam-column joints, *Proceedings 10th International Conference on Structural Faults and Repair*, 2003, London.
18. IS: 456-2000, Plain and reinforced concrete–code of practice, *Bureau of Indian Standard*, New Delhi.
19. Ibarra LF, Ricardo AM, Krawinkler H. Hysteretic models that incorporate strength and stiffness deterioration, *Journal of Earthquake Engineering, Structural Dynamics*, **34**(2005) 1489-511.
20. Rahnama M, Krawinkler H. Effects of soft soil and hystersis model on seismic demands, John A. Blume Earthquake Engineering Center, Department of CEE, *Report No. 108*, 1993 Stanford University, USA.
21. Lakshmanan N. Assesment of repair, Retrofit and Rehabilitation stratigies of reinforced concrete structures, *Proceedings of the National Seminar on Advances in Concrete Technology and Concrete Structures* (ADCONST), 2003, Annamalai University, India, pp. 1-9.
22. Lakshmanan N. Seismic Evaluation and Retrofitting of Buildings and Structures, 26 ISET Annual Lecture, *ISET Journal of Earthquake Technology*, Paper No. 469, Nos. (1-2), **43**(2006) 31-48.